CONF-841121--1

Gas Fluidization of Solids in a Stationary Liquid*

John D. Gabor, John C. Cassulo,
Donna Fountain and James D. Bingle

CONF-841121--1

DE84 006551

Argonne National Laboratory
Reactor Analysis and Safety Division
9700 South Cass Avenue
Argonne, Illinois 60439.

For presentation at the 1984 AIChE Annual Meeting, San Francisco, November 25-29.

*This work was performed under the auspices of the U. S. Department of Energy.

Abstract

Critical gas flow rates were measured for fluidizing initially static beds of particles and for settling of fluidized beds in a stationary pool of liquid. Experiments were conducted with beds of glass, nickel and UO_2 particles ranging in size from 11 to 548 μm in pools of water, ethanol, Freon-113 and water-glycerine solutions. Beds of particles smaller than 328 μm were fluidized by a mechanism of individual particles being carried off of walls of channels in the bed, and beds of particles larger than 328 μm slugged before breaking up to a fluidized state. The data were empirically correlated.

The suspension or fluidization of solid particles in a two-phase gas-liquid fluid has been of considerable interest in chemical processes and recently in nuclear safety analysis. Dhir and Catton [1] and Cho, et al. [2] analyzed heat removal from nuclear core debris assuming fluidization of the particulate debris in boiling coolant. Extensive work has been conducted on three phase fluidization with both the liquid and gas phases flowing [3]. However, in batch processes and certain special situations, such as boiling in a bed of nuclear core debris, gas bubbling through a bed of particles in a non-flowing or stationary pool of liquid must be considered.

The critical gas velocity required to completely suspend or fluidize all of the particles in a stationary pool has had some limited investigation. Kato [4] measured the air velocity to completely fluidize glass spheres (74 to 295 μm) and magnetite particles (74 to 175 μm) in 0.2 N sodium sulfite solution. Kato correlated the data with the following functional relationship:

$$\frac{U_{mf}}{U_m} = f\left[H\, U_m\, (\rho_s - \rho_\ell)/\mu_\ell\right] \qquad (1)$$

Roy, et al. [5] correlated their data in terms of the maximum quantity of solids suspended as a function of the bubble velocity. Their empirically developed correlation depended on the superficial gas Reynolds number, Re_T, based on the tube diameter.

$$H_{max} = 6.84 \times 10^{-4} \left[Re_T\, N_B^{-0.23} \left(\frac{U_t}{U_B}\right)^{-0.18} (\gamma')^{-3}\, C_\mu\right] \qquad Re_T < 500 \qquad (2)$$

$$H_{max} = 1.072 \times 10^{-1} \left[Re_T^{0.2}\, N_B^{-0.23} \left(\frac{U_t}{U_B}\right)^{-0.18} (\gamma')^{-3}\, C_\mu\right] \qquad Re_T < 600 \qquad (3)$$

where $C_\mu = 1 - 0.5892 \log \mu_\ell + 0.1026 \log^2 \mu_\ell$ (μ_ℓ in centipoise).

The data were obtained for various solid materials ranging in size from 127 to 675 μm and water, alcohol, and various oils.

Narayanan et al. [6] considered the minimum gas fluidization velocity as a pickup velocity in which energy is transmitted from the gas phase to the liquid. The velocity to initiate particle suspension was theoretically determined to be:

$$U_{mf} + \frac{1}{3}\left[2g\ H_g\ H_{s\ell}\left(\frac{\rho_\ell - \rho_g}{\rho_\ell}\right)\right]^{1/2} = \left\{2g(\rho_s - \rho_\ell)\left[\frac{2\ D_p}{3\ \rho_\ell} + \frac{H_s\ H_{s\ell}}{\rho_s + H_s\ \rho_\ell}\right]\right\}^{1/2} \quad (4)$$

A correction factor to adjust the theoretical value of U_{mf} to that experimentally observed was empirically correlated as a function of solids concentration.

The gas holdup, H_g, was empirically determined to be:

$$H_g = 0.062\ U \qquad U < 6.7\ \text{cm/s} \quad (5)$$

$$H_g = 0.133\ U^{0.38} \qquad 6.7 < U < 21.34\ \text{cm/s} \quad (6)$$

Their data was based on 84 to 508 μm quartz in water.

Imafuku et al. [7] determined the critical gas velocity to completely suspend the particles in liquid by observing the pressure drop. As for the case of single phase fluidization the pressure drop across the bed increases with gas velocity until the particles are fluidized. After incipient fluidization the pressure drop is independent of gas velocity. They worked with various solid particles ranging from 64 to 180 μm in size and water and glycerine solutions.

While the above cited efforts make a significant contributions in analysis and data, correlations of incipient fluidization in the three-phase system are basically empirical. The mechanisms of transfer of momentum from the gas phase to the liquid and particulate phases are not as simple as for a single-fluid phase flowing through a particle bed. Scheidegger [8] has summarized a considerable amount of work on two-phase flow through packed beds. Tutu, et al. [9] recently experimentally and theoretically analyzed the forces involved in momentum transfer from a flowing gas to beds of 3.18, 6.35, and 12.7 mm stainless steel spheres in a pool of water. These forces include the gas-solid drag, liquid-solid drag, gas-liquid drag, and the surface binding force. This work on two-phase flow through packed beds is not completely applicable to conditions of incipient fluidization. The gas flow through unconfined beds of smaller and less dense particles will force open channels in the bed (this phenomena is described below). This changes the original packing structure and alters the flow distribution through the bed. This structural change as well as the various interacting forces involved severely complicates modelling concepts. However, if the packing remains fixed, the modeling can be simplified. Cho, et al. [2] observed flooding to occur in their bed of rather large dense particles (387 to 650 μm copper) before fluidization began. Therefore, a correlation developed by Wen and Yu [10] for single-phase fluidization could be used since the flooded bed contained essentially no liquid phase. The flooding velocities were calculated using the correlation of Sherwood and Lobo as reformulated by Wallis [11] and were consistently below the observed and calculated incipient fluidization velocities for their copper particle beds.

Where structural changes occur in the bed, i.e., channel formation, correlations of incipient three-phase fluidization are primarily empirical. Implicit in an empirical correlation is its limitation to the range of variables in the data base. This work contributes additional data to expand the data base and observations which should aid in developing models of incipient three-phase fluidization.

Experimental

Experiments were conducted with Lucite columns 49.3, 50 and 100 mm in diameter (see Fig. 1). Beds of 127 to 548-μm glass, 311-μm nickel, and 11-μm UO_2 particles were fluidized. Water, Freon-113, glycerine-water solutions, and ethanol were used for the liquid phase. The liquid level was at least 50 mm above the bed under static conditions (no air flow). In these tests, the incipient fluidization velocities remained the same with this liquid level or higher levels. Air was dispersed at the base of the beds by a 0.312 mm thick sintered stainless steel plate with an average pore opening of 10 μm. Pressure taps were in the plenum beneath the gas distributor plate and at the base of the bed just above the distributor plate. The pressure above the plase was measured with a Statham Laboratories PM6TCb pressure transducer, and the pressure below the plate with a Data Sensors, Inc. PB415 D-10 pressure transducer.

The bed pressure drop was determined with the pressure tap just above the distributor plate. The line to this tap had to be continuously flushed with liquid to keep air bubbles from backing into it. The pressure drop across the distributor plate proved inconsistent from experiment to experiment apparently because of partial capillary clogging of the pores in the distributor plate. The air flow was gradually increased until the bed was fluidized. Fluidization was indicated by observation as well as by the pressure drop leveling off without further increase as the air flow was increased. This behavior, which

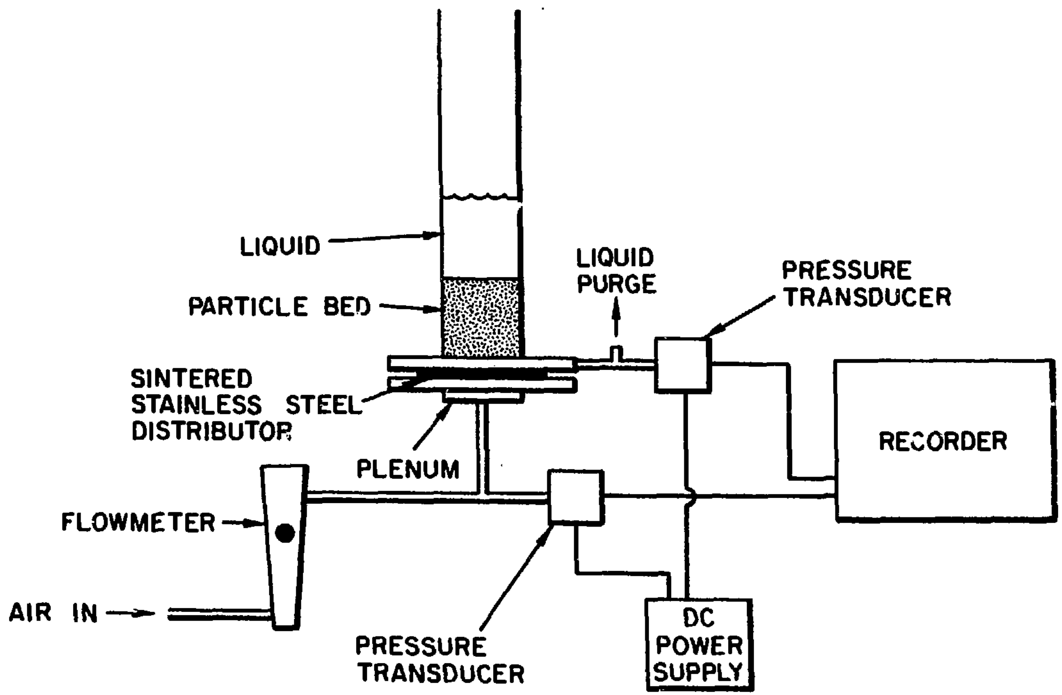

Figure 1. Apparatus for Determining Minimum Fluidization Velocities.

was also observed by Imafuku et al. [7], is identical to fluidization by a single phase fluid. Assuming negligible resistance to air flow by the liquid phase the pressure drop for the fluidized bed is equivalent to the weight of the particle bed. During fluidization the effective density of the liquid phase is increased by the weight of the suspended particles and this is reflected in the pressure at the base.

Results

The minimum fluidization velocity is plotted as a function of static bed depth in Figures 2 to 4. Fig. 2 describes glass-water systems, Fig. 3 glass-Freon-113 systems, and Fig. 4 11-μm UO_2 in water. A complete data tabulation is given in the Appendix. There is a significant difference in behavior between glass particles 327.5 μm in diameter and larger in water and for particles 310 μm and smaller. The incipient fluidization velocity for particles 310 μm in diameter and smaller is independent of bed depth, whereas it is dependent on bed depth for particles 327 μm in diameter and larger.

The air flow forced open channels (~ 5 mm wide) in the particle beds of both large and small particles. For beds of the smaller particles, the particles were stripped off the channel walls until all the particles were suspended. Since the particles were individually removed from the channel walls and carried up into suspension in the liquid pool above the bed, the velocity required for incipient fluidization was independent of the bed depth. However, with larger particles the entire bed was observed to slug up and down off the base before complete breakup to minimum fluidization. Since the entire bed was elevated before large particle fluidization, the incipient fluidization velocity was dependent on bed depth (or bed weight).

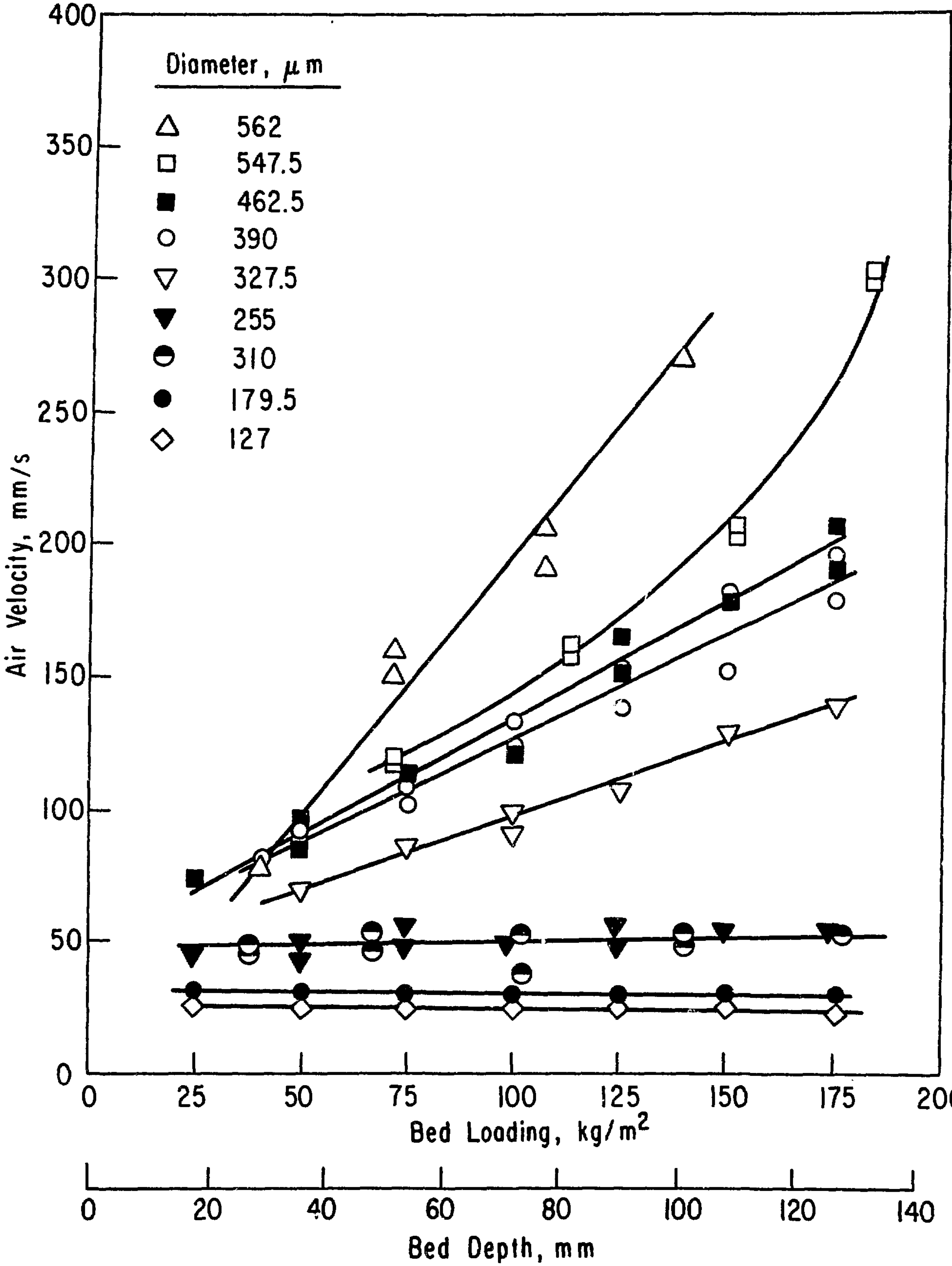

Figure 2. Air Velocities Required to Fluidize Water-Glass Beds.

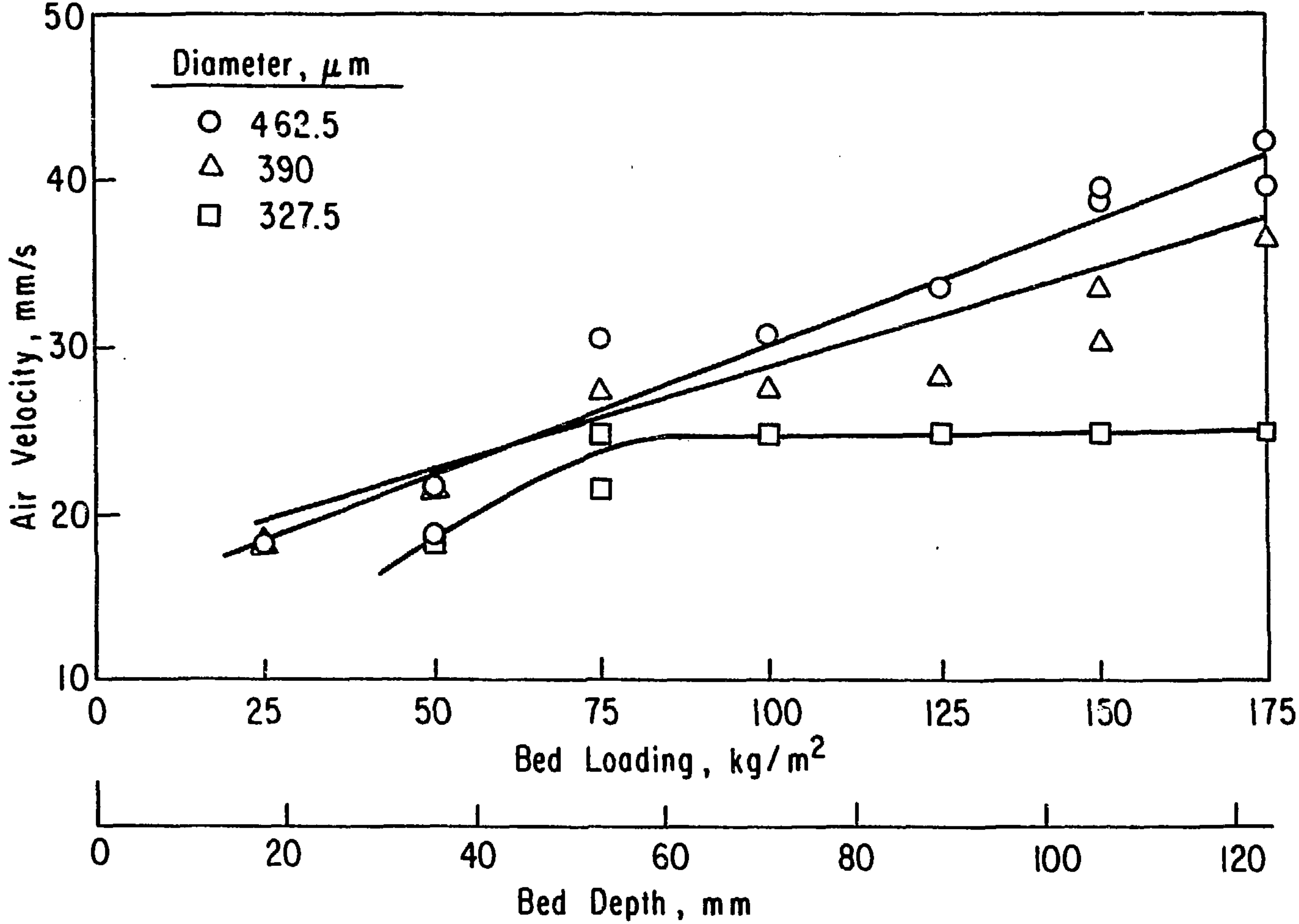

Figure 3. Air Velocities Required to Fluidize Freon-113-Glass Beds.

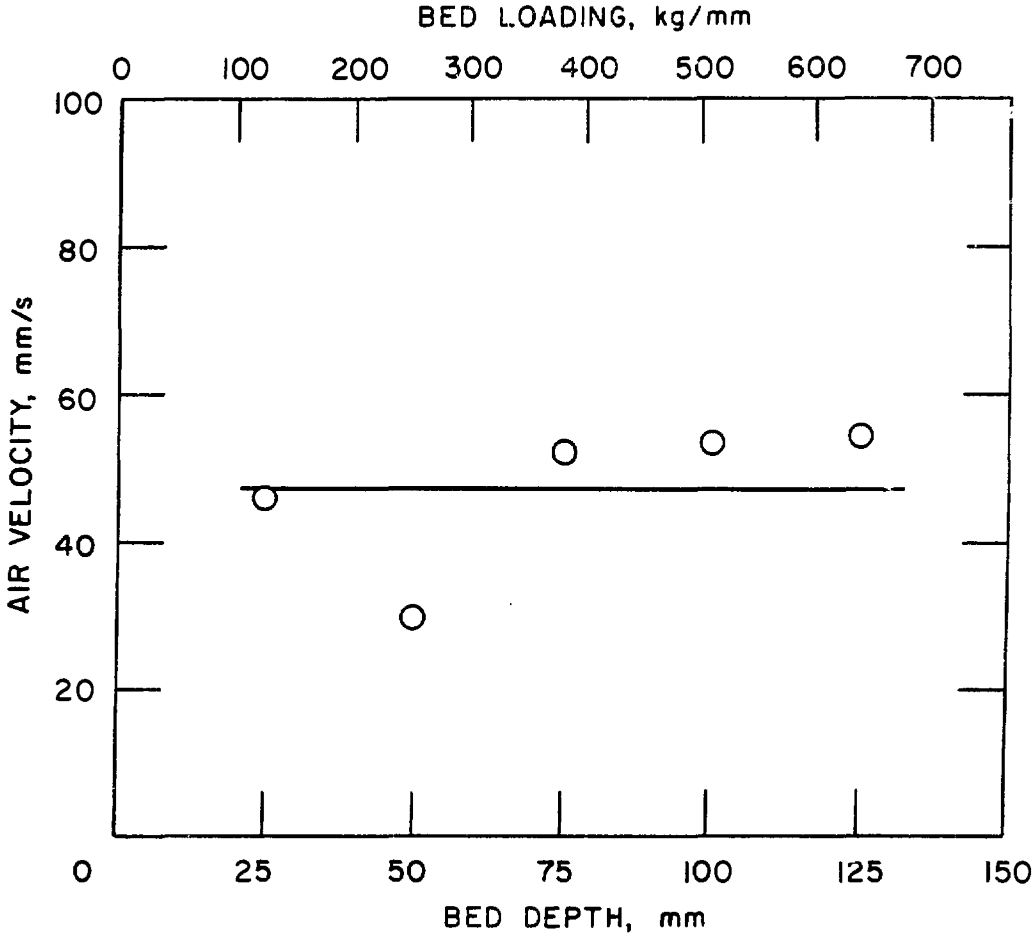

Figure 4. Air Velocities Required to Fluidize Beds of 11 µm UO_2 in Water.

The same behavior was observed with the glass-Freon-113 beds. However, the critical particle diameter of 390 μm was somewhat larger than the 327.5 μm value for the water system. Buoyancy would be greater in the Freon-113, since Freon-113 is denser (1635 Kg/m^3) than water (998 Kg/m^3).

The settling velocity was determined by gradually decreasing the air flow after the particulate phase was completely suspended in the liquid pool. There was a hysteresis effect in that the critical velocity for the transition from a suspended bed to a settled bed was lower than that required to initially fluidize a settled bed.

The fluidization mechanism is too complex for theoretical analysis of incipient fluidization at present. The data were analyzed empirically by determining the effect of each parameter on the minimum fluidization velocity. These parameters were combined in the form of dimensionless groups. For the smaller particles in which the minimum fluidization velocity is independent of bed height the data were correlated by (see Fig. 5):

$$\left(\frac{U_t}{U_{mf}}\right)\left(\frac{U_{mf}\, D_p\, \rho_\ell}{\mu_\ell}\right)^2 = 8.2 \times 10^{-4} \left[\frac{D_p^3\, \rho_\ell\, g(\rho_s-\rho_\ell)}{\mu_\ell^2}\right]^{0.75} \left[\frac{\sigma}{g\, D_p^2(\rho_s-\rho_\ell)}\right]^{0.375} \quad D_p < 328\ \mu m$$

or in terms of dimensionless numbers:

$$\left(\frac{U_t}{U_{mf}}\right) Re_{mf}^{\;2} = 8.2 \times 10^{-4}\, N_f^{\;1.5}\, N_{Eo}^{\;-0.375} \qquad D_p < 328\ \mu m \qquad (7)$$

The coefficient 8.2 x 10^{-4} was determined by regression analysis for a curve with a slope of 1. The best least squares fit resulted in a curve with a slope of 0.97 and a coefficient of 9.5 x 10^{-4}. However, the data scatter does not justify this precision.

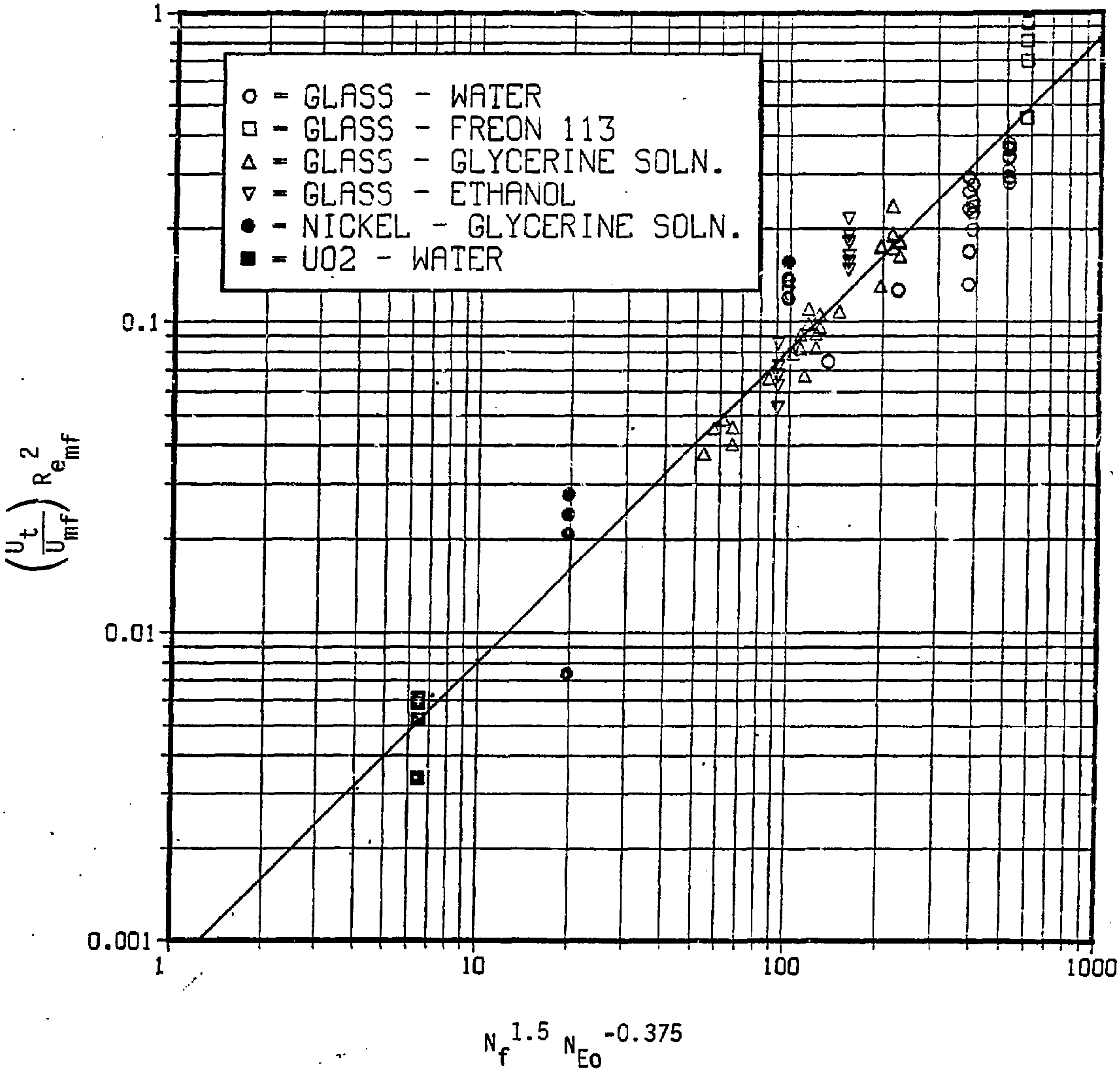

Figure 5. Correlation of Minimum Fluidization of Particles Smaller than 328 μm.

The critical velocity for settling of the particles was correlated by (see Fig. 6):

$$\left(\frac{U_t}{U_{st}}\right) Re_{st}^{2} = 8.67 \times 10^{-5} N_f^{2} N_{Eo}^{-0.50} \qquad D_p < 328 \ \mu m \qquad (8)$$

The critical velocity for settling was not as precisely determined as that for initial fluidization since some judgment was required as to when the fluidized bed began to collapse.

The terminal velocity was calculated from the following:

$$U_t = 0.153 \frac{g^{0.71} D_p^{1.14} (\rho_s - \rho_\ell)^{0.71}}{\rho_\ell^{.29} \mu_\ell^{0.43}} \qquad (9)$$

The correlations (7) and (8) are somewhat similar to

$$C_D Re^2 = \frac{4}{3} N_f^2 \qquad (10)$$

used for determining terminal velocities. Rowe [12] used this functional relationship for correlating the minimum fluidization velocity for the single phase flow of either liquid or gas by correcting the coefficient of friction, C_D, by a factor of 68.5 to account for the presence of the neighboring particles. This is consistent with the observed mechanism of small particle incipient fluidization in which individual particles are stripped from the channel walls until the entire bed is suspended.

The 311 μm nickel particles were somewhat smaller than the smallest size copper particles (387 μm) used in the tests by Cho, et al. [12]. Since both copper and nickel were the same density, it was of interest to apply the flooding criteria given in Wallis [10] to the 311 μm nickel particle bed. The flooding velocity was calculated to be about 0.10 m/s, which is less than

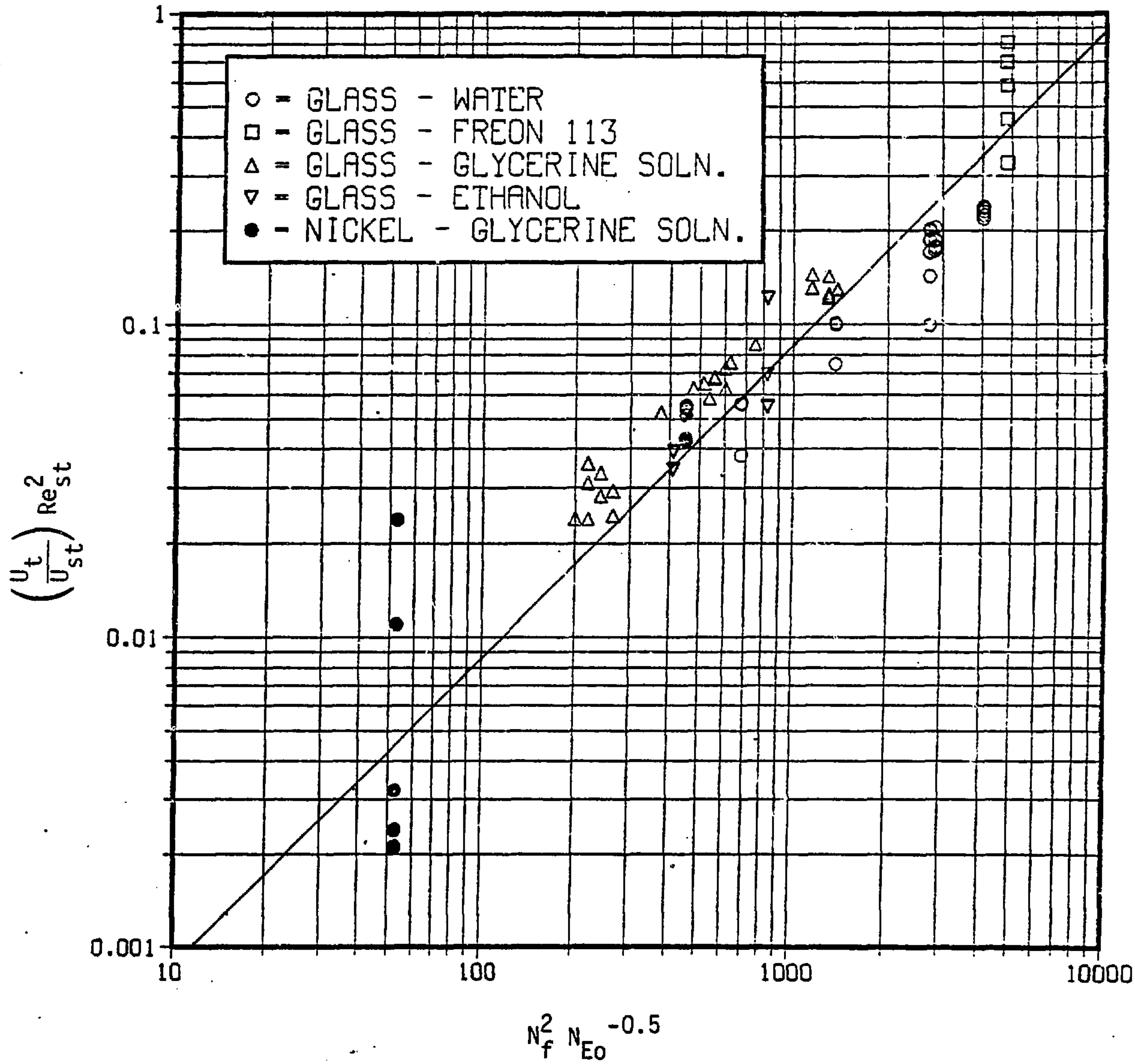

Figure 6. Correlation of Critical Settling Velocities of Particles Less Than 328 μm.

observed fluidization velocities. It should be noted that 311 μm is well below the smallest packing size (6 mm) used for the flooding correlation. The minimum fluidization velocity for the 311 μm nickel particles based on a flooded bed with only air flow through the particle bed, using the Wen and Yu [11] correlation is 0.26 m/s. This was below the observed 0.4 to 0.6 m/s range for the three phase system.

For the larger beds in which the minimum fluidization velocity is dependent on bed height the data were correlated by (see Fig. 7):

$$\left[\frac{\rho_\ell \; U_{mf}^2}{D_p \; g(\rho_s - \rho_\ell)}\right]^{1.75} \left[\frac{D_t^2 g(\rho_s - \rho_\ell)}{U_{mf} \; \mu}\right]^{.5} \left[\frac{gD_p}{U_{mf}^2}\right]^{1.0} = 77.0 \; H^{.5} \qquad D_p > 328 \; \mu m$$

or in terms of dimensionless groups:

$$j^{*\,3.5}_{mf} \; U^{*\,-.5}_{mf} \; Fr_{mf}^{-1.0} = 77.0 \; H^{.5} \qquad D_p > 328 \; \mu m \qquad (11)$$

The above expression can be simplified to:

$$U_{mf} = 77.0 \frac{H^{.5} \; g^{.25} \; D_p^{.75} \; (\rho_s - \rho_\ell)^{1.25}}{\rho_\ell^{1.75} \; D_t \; \mu^{.5}} \qquad D_p > 328 \; \mu m \qquad (12)$$

A least squares analysis indicated that the data would be better correlated with H to the 0.55 power and a constant of 67.9. However, it was felt that the data scatter did not justify this precision. Therefore, a least squares fit was forced to H to the 0.5 power with a resulting constant of 77.0.

The critical velocity for settling of fluidized particles was correlated by (see Fig. 8):

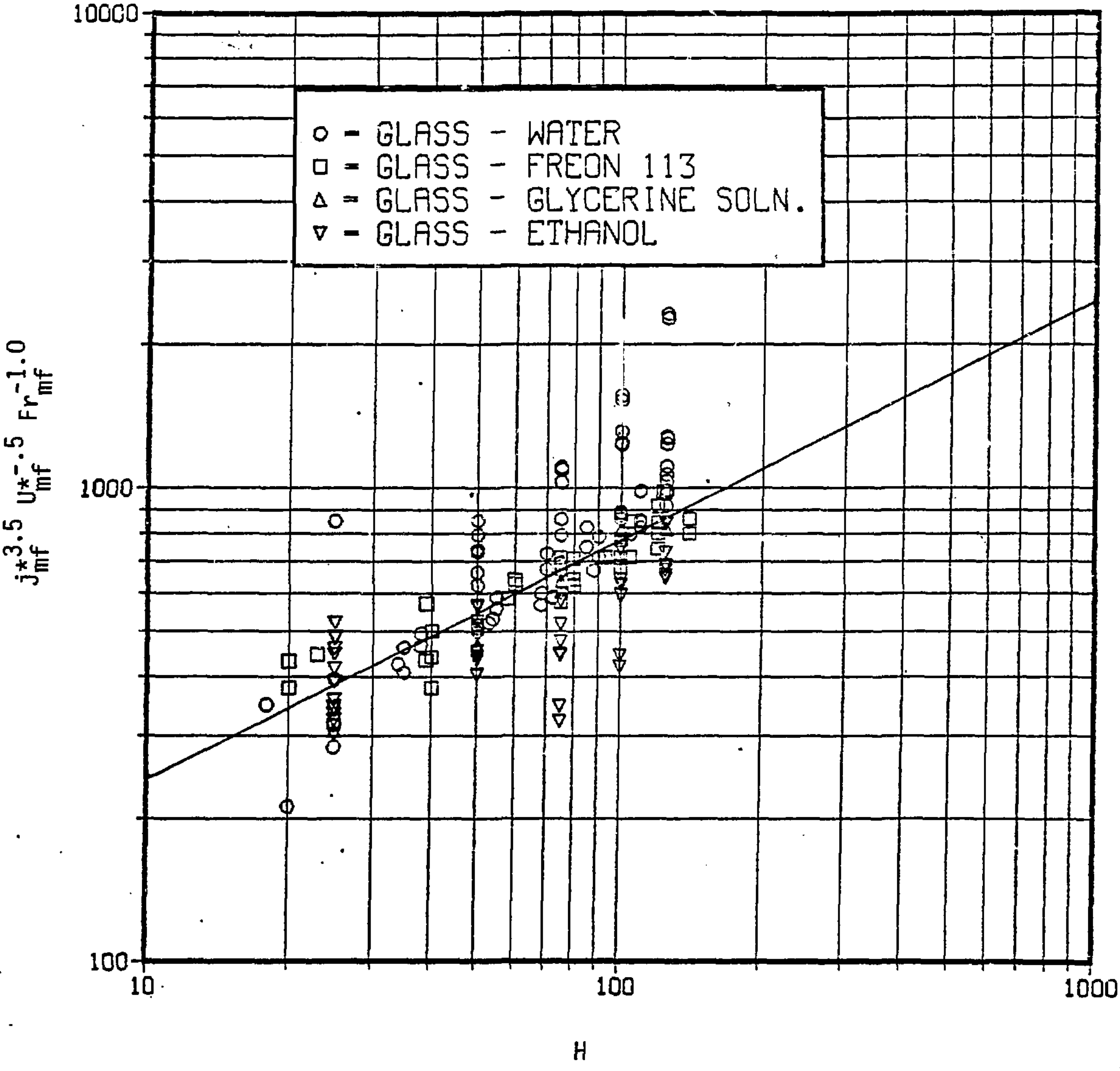

Figure 7. Correlation of Minimum Fluidization of Particles Greater than 328 μm.

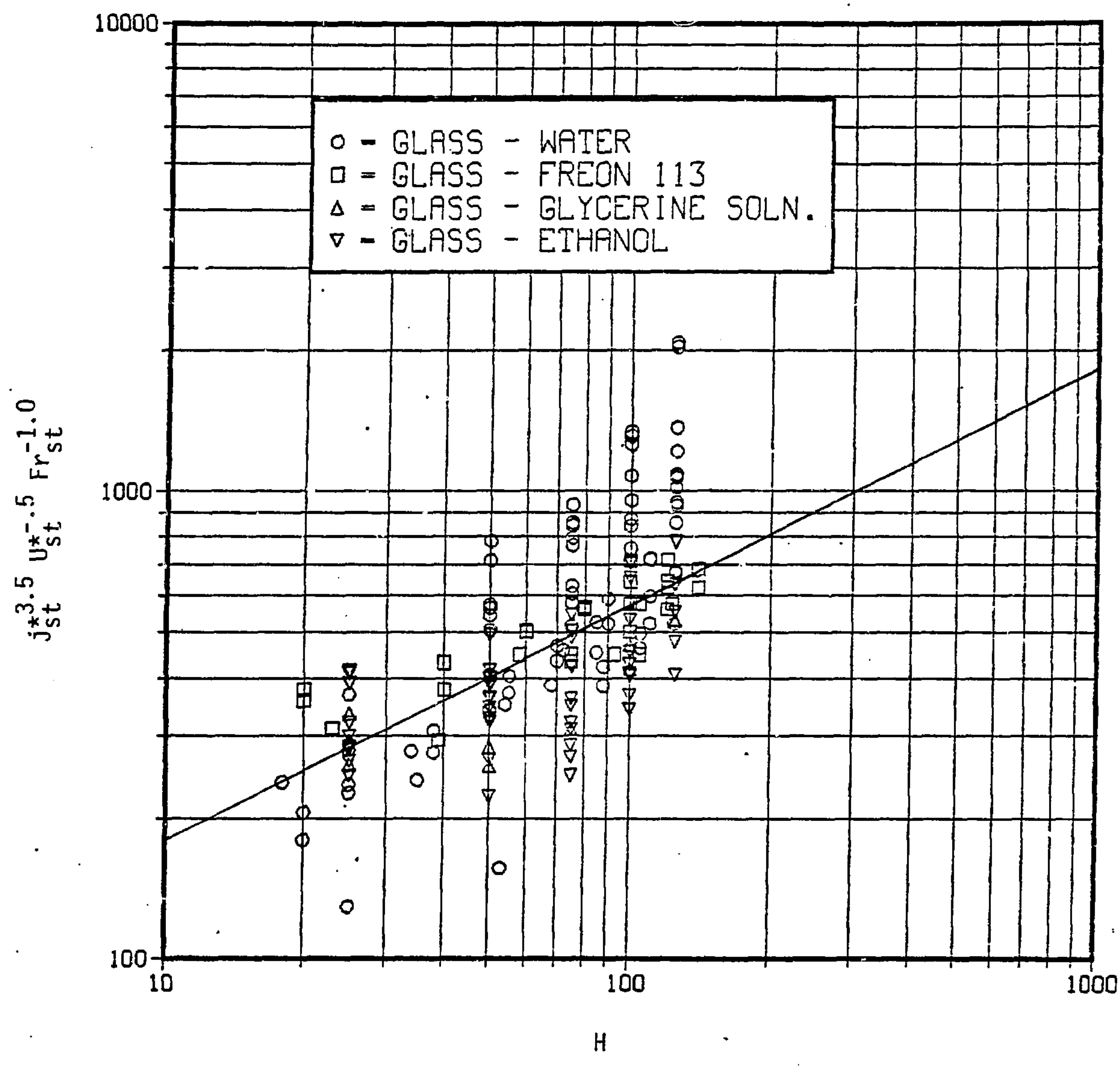

Figure 8. Correlation of Critical Settling Velocities of Particles Greater than 328 μm.

$$j^{*3.5}_{st}\ U^{*-.5}_{st}\ Fr_{st}^{-1.0} = 57.7\ H^{.5} \qquad D_p > 328\ \mu m \qquad (13)$$

which can be rearranged to:

$$U_{st} = 57.7\ \frac{H^{.5}\ g^{.25}\ D_p^{.75}\ (\rho_s-\rho_\ell)^{1.25}}{\rho_\ell^{1.75}\ D_t\mu^{.5}} \qquad D_p > 328\ \mu m \qquad (14)$$

Without force fitting, the least squares analysis yielded H to the 0.57 power and a constant 43.1.

The data scatter was greater for the critical settling velocity than for the minimum fluidization velocity, and the data scatter was greater for the larger particles than for the smaller particles. The onset of fluidization was more catastrophic with the larger particles. The entire bed slugged before breaking up into the fluidized state. The breakup of the slugging bed was not as sharply defined as the smoother process of fluidizing the smaller particles individually. The stability of the particulate slugs was sensitive to the column diameter. Within the range of data scatter, the minimum fluidization velocity was observed to be inversely proportional to the column diameter (to the first power). Narayanan et al. [6] assumed a power of 0.5 for particles greater than 200 μm for their correction factor based on work at slurry transport through pipes. Additional data are needed to confirm the column diameter dependency for three-phase fluidization since the current data are limited to one series of measurements with 548 μm glass particles for two different column diameters.

Conclusions

1. Bed pressure drop increased with increased gas flow and then leveled off after incipient fluidization in a manner similar as for fluidization with a single phase fluid.
2. The critical gas velocity required for fluidization was independent of particle bed depth for particles less than 328 μm. The particles were individually stripped off the channel walls until the entire bed was fluidized.
3. The minimum fluidization gas velocity required for beds of particles larger than 328 μm was dependent on particle bed depth. These beds slugged before breaking up into a fluidized state.
4. Further work is needed on the effect of tube diameter.
5. Further analysis is needed to determine the criterion for beds fluidized by stripping of individual particles off the channel walls and for beds fluidized by breakup of slugging.

NOMENCLATURE

C_D	drag coefficient
C_μ	viscosity correlation factor
D_p	particle diameter
D_t	tube diameter
Fr	Froude number, $U^2/g\ D_p$
g	acceleration due to gravity
H	static particle bed depth
H_g	gas hold up
H_ℓ	static liquid depth
H_{max}	maximum quantity of solids that can be held in suspension
H_s	solids concentration, Kg of solid/Kg of liquid
$H_{s\ell}$	static slurry height
j*	$U\ \rho_\ell^{1/2}\ [g\ D_p\ (\rho_s - \rho_\ell)]^{-1/2}$
L	bed loading, kg/m^2
N_B	modified bubble flow number, $\sigma/U_B\ \mu_\ell$
$N_{E\ddot{o}}$	Eötvös number, $g\ D_p^{\ 2}\ (\rho_s - \rho_\ell)/\sigma$
N_f	inverse viscosity, $[D_p^{\ 3}\ \rho_\ell\ g\ (\rho_s - \rho_\ell)]^{1/2}/\mu_\ell$
Re	Reynolds number, $U\ D_p\ \rho_\ell/\mu_\ell$
Re_T	$U\ D_T\ \rho_\ell/\mu_\ell$
U	superficial gas velocity
U*	$U\ \mu/D_t^2\ g\ (\rho_s - \rho_\ell)$
U_B	bubble velocity
U_m	terminal velocity of largest particle
U_t	particle terminal velocity in liquid phase
ε	particle bed voidage

γ wettability factor

γ' γ less wettable solid/γ most wettable solid

μ_ℓ liquid density

ρ_g gas density

ρ_ℓ liquid density

ρ_s particle density

σ surface tension

ψ shape factor

Subscripts

m_f minimum fluidization

st settling

References

1. Dhir, V. and I. Catton, "Dryout Heat Fluxes for Inductively Heated Particulate Beds," Paper 75-WA/HT-19, ASME Winter Annual Meeting, Houston (1975).

2. Cho, D. H., L. J. Stachyra and G. A. Lambert, "Fludization Considerations in Debris Bed Heat Removal," Trans. Am. Nucl. Soc., 38, 383 (1981).

3. Epstein, N., "Three-phase Fluidization: Some Knowledge Gaps," Can. J. Chem. Eng., 59, 649 (1981).

4. Kato, Y., "Gas-liquid Contact in a Gas-liquid-solid Fluidized Bed," Kagaku Kogaku (Abridged edition), 1, 3 (1963).

5. Roy, N. K., D. K. Guha and M. N. Rao, "Suspension of Solids in a Bubbling Liquid," Chem. Eng. Sci., 19, 215 (1964).

6. Narayanan, S., V. K. Bhatia and D. K. Guha, "Suspension of Solids by Bubble Agitation," Can. J. Chem. Eng., 47, 360 (1969).

7. Imafuku, K., T. Y. Wang, K. Koide and H. Kubata, "The Behavior of Suspended Solid Particles in the Bubble Column," J. Chem. Eng. Japan, 1, 153 (1968).

8. A. E. Scheidegger, "The Physics of Flow Through Porous Media," 3rd Edition, University of Toronto Press, Toronto, 1974.

9. N. K. Tutu, T. Ginsgerg, and J. C. Chen, "Interfacial Drag for Two-phase Flow Through High-Permeability Porous Beds," paper presented at 21st AIChE/ASME National Heat Transfer Conference, Seattle (1983).

10. G. B. Wallis, "One-Dimensional Two-Phase Flow," McGraw-Hill, New York, p. 338 (1969).

11. C. Y. Wen and Y. H. Yu, "Mechanics of Fluidization," CEP Progress Symposium Series No. 62, Vol. 62, 100 (1966).

12. Rowe, P. N., "Drag Force in a Hydraulic Model of a Fluidized Bed - Part II," Trans. of the Institute of Chemical Engineer, 39, 43 (1961).

APPENDIX

Table Al. Three-Phase Minimum Fluidization and Settling Velocities

Test No.	D_p,mm	ρ_s, Kg/ms	Ψ	Dt,mm	H,mm	L, Kg/m^2	ϵ	H_ℓ,mm	ρ_ℓ, Kg/m^3	μ_ℓ,Cp	σ, dynes/cm	U_{mf}, cm/s	U_{st}, cm/s
1	255.0	2600	1.0	49.8	18.0	25.63	.4	118.0	997.1	.894	71.97	4.03	2.98
2	255.0	2600	1.0	49.8	18.0	25.63	.4	118.0	997.1	.894	71.97	4.04	3.49
3	255.0	2600	1.0	49.8	40.0	51.27	.4	140.0	997.1	.894	71.97	4.59	2.50
4	255.0	2600	1.0	49.8	40.0	51.27	.4	140.0	997.1	.894	71.97	4.05	2.98
5	255.0	2600	1.0	49.8	60.0	76.90	.4	160.0	997.1	.894	71.97	5.13	3.50
6	255.0	2600	1.0	49.8	60.0	76.90	.4	160.0	997.1	.894	71.97	4.60	3.51
7	255.0	2600	1.0	49.8	20.0	25.63	.4	120.0	997.1	.894	71.97	2.94	1.74
8	255.0	2600	1.0	49.8	20.0	25.63	.4	120.0	997.1	.894	71.97	2.31	1.73
9	255.0	2600	1.0	49.8	40.0	51.27	.4	140.0	997.1	.894	71.97	2.96	1.74
10	255.0	2600	1.0	49.8	40.0	51.27	.4	140.0	997.1	.894	71.97	2.96	1.74
11	255.0	2600	1.0	49.8	55.0	76.90	.4	155.0	997.1	.894	71.97	2.97	1.74
12	255.0	2600	1.0	49.8	55.0	76.90	.4	155.0	997.1	.894	71.97	2.97	1.74
13	255.0	2600	1.0	49.8	70.0	102.54	.4	170.0	997.1	.894	71.97	4.59	3.51
14	255.0	2600	1.0	49.8	90.0	128.17	.4	190.0	997.1	.894	71.97	4.59	3.25
15	255.0	2600	1.0	49.8	90.0	128.17	.4	190.0	997.1	.894	71.97	5.10	3.25
16	255.0	2600	1.0	49.8	110.0	153.80	.4	210.0	997.1	.894	71.97	5.14	3.27
17	255.0	2600	1.0	49.8	110.0	153.80	.4	210.0	997.1	.894	71.97	5.14	3.53
18	255.0	2600	1.0	49.8	125.0	179.44	.4	225.0	997.1	.894	71.97	5.13	3.52
19	255.0	2600	1.0	49.8	125.0	179.44	.4	225.0	997.1	.894	71.97	5.13	3.52
20	426.0	2600	1.0	49.8	25.0	38.96	.4	125.0	997.1	.894	71.97	6.21	5.04
21	426.0	2600	1.0	49.8	25.0	38.96	.4	125.0	997.1	.894	71.97	7.14	5.21
22	426.0	2600	1.0	49.8	50.0	73.93	.4	150.0	997.1	.894	71.97	12.35	10.37
23	426.0	2600	1.0	49.8	50.0	73.93	.4	150.0	997.1	.894	71.97	14.36	9.80
24	426.0	2600	1.0	49.8	75.0	119.25	.4	175.0	997.1	.894	71.97	18.55	15.24
25	426.0	2600	1.0	49.8	75.0	119.25	.4	175.0	997.1	.894	71.97	19.72	16.86
26	426.0	2600	1.0	49.8	100.0	143.34	.4	200.0	997.1	.894	71.97	28.23	24.19
27	426.0	2600	1.0	49.8	100.0	143.34	.4	200.0	997.1	.894	71.97	27.63	22.82
28	426.0	2600	1.0	49.8	125.0	183.44	.4	225.0	997.1	.894	71.97	41.70	37.50
29	426.0	2600	1.0	49.8	125.0	183.44	.4	225.0	997.1	.894	71.97	40.89	36.81
30	260.0	2600	1.0	49.8	25.0	34.55	.4	125.0	997.1	.894	71.97	3.41	3.21
31	260.0	2600	1.0	49.8	25.0	34.55	.4	125.0	997.1	.894	71.97	3.35	3.19
32	260.0	2600	1.0	49.8	50.0	71.47	.4	150.0	997.1	[illegible]	71.97	3.33	3.19
33	260.0	2600	1.0	49.8	50.0	71.47	.4	150.0	997.1	[illegible]	71.97	4.06	3.51
34	260.0	2600	1.0	49.8	75.0	110.33	.4	175.0	997.1	.894	71.97	4.04	3.19
35	260.0	2600	1.0	49.8	75.0	110.33	.4	175.0	997.1	.894	71.97	3.82	2.97
36	260.0	2600	1.0	49.8	100.0	145.45	.4	200.0	997.1	.894	71.97	4.76	3.03
37	260.0	2600	1.0	49.8	100.0	145.45	.4	200.0	997.1	.894	71.97	4.20	3.21
38	260.0	2600	1.0	49.8	125.0	180.21	.4	225.0	997.1	.894	71.97	3.87	3.05
39	260.0	2600	1.0	49.8	125.0	180.21	.4	225.0	997.1	.894	71.97	4.21	3.21
40	548.0	2600	1.0	49.8	25.0	40.14	.4	175.0	997.1	.894	71.97	6.21	2.82
41	548.0	2600	1.0	49.8	25.0	40.14	.4	175.0	997.1	.894	71.97	6.21	2.82
42	548.0	2600	1.0	49.8	50.0	73.72	.4	200.0	997.1	.894	71.97	11.22	7.42
43	548.0	2600	1.0	49.8	50.0	73.72	.4	200.0	997.1	.894	71.97	11.25	7.46
44	548.0	2600	1.0	49.8	75.0	115.97	.4	225.0	997.1	.894	71.97	15.16	12.62
45	548.0	2600	1.0	49.8	75.0	115.97	.4	225.0	997.1	.894	71.97	14.88	11.22
46	548.0	2600	1.0	49.8	100.0	154.98	.4	250.0	997.1	.894	71.97	19.35	16.49
47	548.0	2600	1.0	49.8	100.0	154.98	.4	250.0	997.1	.894	71.97	19.40	16.49
48	548.0	2600	1.0	49.8	125.0	187.38	.4	275.0	997.1	.894	71.97	22.50	20.60
49	548.0	2600	1.0	49.8	125.0	187.38	.4	275.0	997.1	.894	71.97	22.50	22.22
50	548.0	2600	1.0	49.8	25.0	40.14	.4	125.0	997.1	.894	71.97	6.92	8.05
51	548.0	2600	1.0	49.8	50.0	73.72	.4	150.0	997.1	.894	[illegible]	11.09	8.87
52	548.0	2600	1.0	49.8	50.0	73.72	.4	150.0	997.1	.894	[illegible]	10.29	8.83
53	548.0	2600	1.0	49.8	75.0	115.97	.4	175.0	997.1	.894	71.97	15.04	13.71
54	548.0	2600	1.0	49.8	75.0	115.97	.4	175.0	997.1	.894	71.97	14.52	13.19
55	548.0	2600	1.0	49.8	100.0	154.98	.4	200.0	997.1	.894	71.97	19.11	18.38
56	548.0	2600	1.0	49.8	100.0	154.98	.4	200.0	997.1	.894	71.97	18.80	19.00
57	548.0	2600	1.0	49.8	125.0	187.38	.4	225.0	997.1	.894	71.97	27.86	29.35
58	548.0	2600	1.0	49.8	125.0	187.38	.4	225.0	997.1	.894	71.97	27.66	26.53

Test No.	D_p,mm	ρ_s, Kg/ms	Ψ	Dt,mm	H,mm	L, Kg/m^2	ϵ	H_ℓ,mm	ρ_ℓ, Kg/m^3	μ_ℓ,Cp	σ, dynes/cm	U_{mf}, cm/s	U_{st}, cm/s
59	127.0	2600	1.0	49.8	20.0	25.63	.4	120.0	997.1	.894	71.97	2.36	1.77
60	127.0	2600	1.0	49.8	35.0	51.27	.4	135.0	997.1	.894	71.97	2.36	1.78
61	127.0	2600	1.0	49.8	55.0	76.90	.4	155.0	997.1	.894	71.97	2.37	1.78
62	127.0	2600	1.0	49.8	55.0	76.90	.4	155.0	997.1	.894	71.97	2.37	1.78
63	127.0	2600	1.0	49.8	75.0	102.54	.4	175.0	997.1	.894	71.97	2.37	1.78
64	127.0	2600	1.0	49.8	90.0	128.17	.4	190.0	997.1	.894	71.97	2.37	1.21
65	127.0	2600	1.0	49.8	90.0	128.17	.4	190.0	997.1	.894	71.97	2.37	1.21
66	127.0	2600	1.0	49.8	108.0	153.80	.4	208.0	997.1	.894	71.97	2.37	1.21
67	127.0	2600	1.0	49.8	108.0	153.80	.4	208.0	997.1	.894	71.97	2.38	1.21
68	127.0	2600	1.0	49.8	120.0	179.44	.4	220.0	997.1	.894	71.97	2.37	1.21
69	127.0	2600	1.0	49.8	120.0	179.44	.4	220.0	997.1	.894	71.97	2.38	1.21
70	180.0	2600	1.0	49.8	20.0	25.63	.4	120.0	997.1	.894	71.97	2.38	1.21
71	180.0	2600	1.0	49.8	37.0	51.27	.4	137.0	997.1	.894	71.97	2.97	1.76
72	180.0	2600	1.0	49.8	53.0	76.90	.4	153.0	997.1	.894	71.97	2.97	2.35
73	180.0	2600	1.0	49.8	70.0	102.54	.4	170.0	997.1	.894	71.97	2.99	2.36
74	180.0	2600	1.0	49.8	90.0	128.17	.4	190.0	997.1	.894	71.97	2.99	2.37
75	180.0	2600	1.0	49.8	110.0	153.80	.4	210.0	997.1	.894	71.97	3.00	2.37
76	180.0	2600	1.0	49.8	120.0	179.44	.4	220.0	997.1	.894	71.97	3.00	2.38
77	310.0	2600	1.0	49.8	25.0	38.66	.4	125.0	997.1	.894	71.97	3.01	2.38
78	310.0	2600	1.0	49.8	25.0	38.66	.4	125.0	997.1	.894	71.97	4.56	3.47
79	310.0	2600	1.0	49.8	50.0	68.29	.4	150.0	997.1	.894	71.97	4.31	3.47
80	310.0	2600	1.0	49.8	50.0	68.29	.4	150.0	997.1	.894	71.97	5.00	3.39
81	310.0	2600	1.0	49.8	75.0	105.00	.4	175.0	997.1	.894	71.97	4.36	3.47
82	310.0	2600	1.0	49.8	75.0	105.00	.4	175.0	997.1	.894	71.97	5.04	3.52
83	310.0	2600	1.0	49.8	100.0	144.47	.4	200.0	997.1	.894	71.97	4.16	3.21
84	310.0	2600	1.0	49.8	100.0	144.47	.4	200.0	997.1	.894	71.97	5.08	3.31
85	310.0	2600	1.0	49.8	125.0	181.64	.4	225.0	997.1	.894	71.97	5.33	3.29
86	310.0	2600	1.0	49.8	125.0	181.64	.4	225.0	997.1	.894	71.97	5.57	3.29
87	562.0	2600	1.0	49.8	25.0	41.58	.4	125.0	997.1	.894	71.97	5.42	3.47
88	562.0	2600	1.0	49.8	25.0	41.58	.4	125.0	997.1	.894	71.97	7.42	5.04
89	562.0	2600	1.0	49.8	50.0	73.42	.4	150.0	997.1	.894	71.97	7.14	5.25
90	562.0	2600	1.0	49.8	50.0	73.42	.4	150.0	997.1	.894	71.97	13.87	12.54
91	562.0	2600	1.0	49.8	75.0	109.30	.4	175.0	997.1	.894	71.97	14.72	11.22
92	562.0	2600	1.0	49.8	75.0	109.30	.4	175.0	997.1	.894	71.97	17.66	17.66
93	562.0	2600	1.0	49.8	100.0	141.72	.4	200.0	997.1	.894	71.97	19.11	17.04
94	463.0	2600	1.0	49.8	18.0	25.63	.4	118.0	997.1	.894	71.97	29.16	29.22
95	463.0	2600	1.0	49.8	35.0	51.27	.4	135.0	997.1	.894	71.97	6.71	4.59
96	463.0	2600	1.0	49.8	35.0	51.27	.4	135.0	997.1	.894	71.97	6.86	4.64
97	463.0	2600	1.0	49.8	53.0	76.90	.4	153.0	997.1	.894	71.97	7.83	4.64
98	463.0	2600	1.0	49.8	72.0	102.54	.4	172.0	997.1	.894	71.97	10.00	3.00
99	463.0	2600	1.0	49.8	72.0	102.54	.4	172.0	997.1	.894	71.97	11.29	8.80
100	463.0	2600	1.0	49.8	90.0	128.17	.4	190.0	997.1	.894	71.97	11.33	8.80
101	463.0	2600	1.0	49.8	90.0	128.17	.4	190.0	997.1	.894	71.97	15.15	11.32
102	463.0	2600	1.0	49.8	110.0	153.80	.4	210.0	997.1	.894	71.97	13.71	10.00
103	463.0	2600	1.0	49.8	110.0	153.80	.4	210.0	997.1	.894	71.97	16.42	13.83
104	463.0	2600	1.0	49.8	125.0	179.44	.4	225.0	997.1	.894	71.97	16.35	13.79
105	463.0	2600	1.0	49.8	125.0	179.44	.4	225.0	997.1	.894	71.97	17.70	16.45
106	390.0	2600	1.0	49.8	20.0	25.63	.4	125.0	997.1	.894	71.97	19.01	17.87
107	390.0	2600	1.0	49.8	33.0	51.27	.4	136.0	997.1	.894	71.97	3.58	3.04
108	390.0	2600	1.0	49.8	38.0	51.27	.4	138.0	997.1	.894	71.97	8.36	5.21
109	390.0	2600	1.0	49.8	55.0	76.90	.4	155.0	997.1	.894	71.97	7.86	4.67
110	390.0	2600	1.0	49.8	55.0	76.90	.4	155.0	997.1	.894	71.97	9.94	6.83
111	390.0	2600	1.0	49.8	70.0	102.54	.4	170.0	997.1	.894	71.97	9.42	6.30
112	390.0	2600	1.0	49.8	70.0	102.54	.4	170.0	997.1	.894	71.97	12.25	7.91
113	390.0	2600	1.0	49.8	85.0	128.17	.4	185.0	997.1	.894	71.97	11.36	7.35
114	390.0	2600	1.0	49.8	85.0	128.17	.4	185.0	997.1	.894	71.97	12.67	7.65
115	390.0	2600	1.0	49.8	110.0	153.80	.4	210.0	997.1	.894	71.97	13.96	8.87
116	390.0	2600	1.0	49.8	110.0	153.80	.4	210.0	997.1	.894	71.97	16.66	10.10
117	390.0	2600	1.0	49.8	125.0	179.44	.4	225.0	997.1	.894	71.97	13.97	8.82
118	390.0	2600	1.0	49.8	125.0	179.44	.4	225.0	997.1	.894	71.97	16.02	11.43
119	328.0	2600	1.0	49.8	20.0	25.63	.4	120.0	997.1	.894	71.97	16.42	11.39
120	328.0	2600	1.0	49.8	34.0	51.27	.4	134.0	997.1	.894	71.97	0.00	3.06
121	328.0	2600	1.0	49.8	34.0	51.27	.4	134.0	997.1	.894	71.97	6.30	4.13
122	328.0	2600	1.0	49.8	54.0	76.90	.4	154.0	997.1	.894	71.97	6.30	4.13
123	328.0	2600	1.0	49.8	54.0	76.90	.4	154.0	997.1	.894	71.97	7.88	5.21
												7.83	5.21

TABLE A1. (cont'd)

Test No.	D_p, mm	ρ_s, Kg/ms	Ψ	Dt, mm	H, mm	L, Kg/m^2	ε	H_ℓ, mm	ρ_ℓ, Kg/m^3	μ_ℓ, Cp	σ, dynes/cm	U_{mf}, cm/s	U_{st}, cm/s
124	328.0	2600	1.0	49.8	68.0	102.54	.4	168.0	997.1	.894	71.97	8.42	5.75
125	328.0	2600	1.0	49.8	68.0	102.54	.4	168.0	997.1	.894	71.97	8.91	5.74
126	328.0	2600	1.0	49.8	88.0	128.17	.4	188.0	997.1	.894	71.97	9.93	6.28
127	328.0	2600	1.0	49.8	88.0	128.17	.4	188.0	997.1	.894	71.97	9.93	5.73
128	328.0	2600	1.0	49.8	105.0	153.80	.4	205.0	997.1	.894	71.97	11.89	6.97
129	328.0	2600	1.0	49.8	105.0	153.80	.4	205.0	997.1	.894	71.97	11.89	7.36
130	328.0	2600	1.0	49.8	124.0	179.44	.4	224.0	997.1	.894	71.97	12.79	7.71
131	328.0	2600	1.0	49.8	124.0	179.44	.4	224.0	997.1	.894	71.97	12.79	7.71
132	390.0	2600	1.0	49.8	23.0	25.63	.4	123.0	1564.8	.680	17.30	1.73	1.21
133	390.0	2600	1.0	49.8	39.0	51.27	.4	139.0	1564.8	.680	17.30	1.68	1.14
134	390.0	2600	1.0	49.8	39.0	51.27	.4	139.0	1564.8	.680	17.30	2.22	1.14
135	390.0	2600	1.0	49.8	58.0	76.90	.4	158.0	1564.8	.680	17.30	2.27	1.74
136	390.0	2600	1.0	49.8	58.0	76.90	.4	158.0	1564.8	.680	17.30	2.27	1.74
137	390.0	2600	1.0	49.8	75.0	102.54	.4	175.0	1564.8	.680	17.30	2.23	1.74
138	390.0	2600	1.0	49.8	75.0	102.54	.4	175.0	1564.8	.680	17.30	2.76	1.68
139	390.0	2600	1.0	49.8	93.0	128.17	.4	193.0	1564.8	.680	17.30	2.77	1.74
140	390.0	2600	1.0	49.8	93.0	128.17	.4	193.0	1564.8	.680	17.30	2.76	1.74
141	390.0	2600	1.0	49.8	105.0	153.80	.4	205.0	1564.8	.680	17.30	3.30	1.74
142	390.0	2600	1.0	49.8	105.0	153.80	.4	205.0	1564.8	.680	17.30	2.77	2.23
143	390.0	2600	1.0	49.8	123.0	179.44	.4	223.0	1564.8	.680	17.30	3.82	2.23
144	390.0	2600	1.0	49.8	123.0	179.44	.4	223.0	1564.8	.680	17.30	3.82	2.23
145	390.0	2600	1.0	49.8	20.0	25.63	.4	120.0	1564.8	.680	17.30	1.67	1.39
146	390.0	2600	1.0	49.8	40.0	51.27	.4	140.0	1564.8	.680	17.30	1.94	1.67
147	390.0	2600	1.0	49.8	40.0	51.27	.4	140.0	1564.8	.680	17.30	1.94	1.67
148	390.0	2600	1.0	49.8	60.0	76.90	.4	160.0	1564.8	.680	17.30	2.48	1.94
149	390.0	2600	1.0	49.8	60.0	76.90	.4	160.0	1564.8	.680	17.30	2.48	1.94
150	390.0	2600	1.0	49.8	80.0	102.54	.4	180.0	1564.8	.680	17.30	2.49	2.20
151	390.0	2600	1.0	49.8	80.0	102.54	.4	180.0	1564.8	.680	17.30	2.75	2.20
152	390.0	2600	1.0	49.8	100.0	128.17	.4	200.0	1564.8	.680	17.30	3.02	2.49
153	390.0	2600	1.0	49.8	100.0	128.17	.4	200.0	1564.8	.680	17.30	3.02	2.49
154	390.0	2600	1.0	49.8	100.0	153.80	.4	200.0	1564.8	.680	17.30	3.02	2.23
155	390.0	2600	1.0	49.8	100.0	153.80	.4	200.0	1564.8	.680	17.30	2.76	2.76
156	390.0	2600	1.0	49.8	120.0	179.44	.4	220.0	1564.8	.680	17.30	3.56	2.50
157	390.0	2600	1.0	49.8	120.0	179.44	.4	220.0	1564.8	.680	17.30	3.28	2.77
158	328.0	2600	1.0	49.8	20.0	25.63	.4	120.0	1564.8	.680	17.30	1.09	.79
159	328.0	2600	1.0	49.8	45.0	51.27	.4	145.0	1564.8	.680	17.30	1.67	1.09
160	328.0	2600	1.0	49.8	45.0	51.27	.4	145.0	1564.8	.680	17.30	1.67	1.40
161	328.0	2600	1.0	49.8	60.0	76.90	.4	160.0	1564.8	.680	17.30	1.94	1.40
162	328.0	2600	1.0	49.8	60.0	76.90	.4	160.0	1564.8	.680	17.30	2.21	1.67
163	328.0	2600	1.0	49.8	80.0	102.54	.4	180.0	1564.8	.680	17.30	2.21	1.67
164	328.0	2600	1.0	49.8	80.0	102.54	.4	180.0	1564.8	.680	17.30	2.21	1.68
165	328.0	2600	1.0	49.8	100.0	128.17	.4	200.0	1564.8	.680	17.30	2.22	1.67
166	328.0	2600	1.0	49.8	100.0	128.17	.4	200.0	1564.8	.680	17.30	2.22	1.67
167	328.0	2600	1.0	49.8	120.0	153.80	.4	220.0	1564.8	.680	17.30	2.22	1.94
168	328.0	2600	1.0	49.8	120.0	153.80	.4	220.0	1564.8	.680	17.30	2.22	1.67
169	328.0	2600	1.0	49.8	135.0	179.44	.4	235.0	1564.8	.680	17.30	2.22	1.40
170	328.0	2600	1.0	49.8	135.0	179.44	.4	235.0	1564.8	.680	17.30	2.22	1.68
171	463.0	2600	1.0	49.8	20.0	25.63	.4	120.0	1564.8	.680	17.30	1.67	1.67
172	463.0	2600	1.0	49.8	40.0	51.27	.4	140.0	1564.8	.680	17.30	1.67	1.67
173	463.0	2600	1.0	49.8	40.0	51.27	.4	140.0	1564.8	.680	17.30	1.94	1.67
174	463.0	2600	1.0	49.8	60.0	76.90	.4	160.0	1564.8	.680	17.30	2.76	2.22
175	463.0	2600	1.0	49.8	60.0	76.90	.4	160.0	1564.8	.680	17.30	2.76	2.22
176	463.0	2600	1.0	49.8	80.0	102.54	.4	180.0	1564.8	.680	17.30	2.75	2.47
177	463.0	2600	1.0	49.8	80.0	102.54	.4	180.0	1564.8	.680	17.30	2.74	2.47
178	463.0	2600	1.0	49.8	100.0	128.17	.4	200.0	1564.8	.680	17.30	3.01	2.71
179	463.0	2600	1.0	49.8	100.0	128.17	.4	200.0	1564.8	.680	17.30	3.00	0.00
180	463.0	2600	1.0	49.8	120.0	153.80	.4	220.0	1564.8	.680	17.30	3.54	2.47
181	463.0	2600	1.0	49.8	120.0	153.80	.4	220.0	1564.8	.680	17.30	3.28	2.75
182	463.0	2600	1.0	49.8	140.0	179.44	.4	240.0	1564.8	.680	17.30	3.54	3.01
183	463.0	2600	1.0	49.8	140.0	179.44	.4	240.0	1564.8	.680	17.30	3.80	2.75
184	548.0	2600	1.0	100.0	25.0	37.98	.4	125.0	997.1	.894	71.97	9.25	0.00
185	548.0	2600	1.0	100.0	50.0	75.82	.4	150.0	997.1	.894	71.97	7.93	7.74
186	548.0	2600	1.0	100.0	50.0	75.82	.4	150.0	997.1	.894	71.97	9.27	8.49
187	548.0	2600	1.0	100.0	75.0	114.00	.4	175.0	997.1	.894	71.97	11.97	9.29
188	548.0	2600	1.0	100.0	100.0	147.91	.4	200.0	997.1	.894	71.97	13.47	10.37
189	548.0	2600	1.0	100.0	100.0	147.91	.4	200.0	997.1	.894	71.97	13.39	11.73

Test No.	D_p, mm	ρ_s, Kg/ms	Ψ	Dt, mm	H, mm	L, Kg/m^2	ε	H_ℓ, mm	ρ_ℓ, Kg/m^3	μ_ℓ, Cp	σ, dynes/cm	U_{mf}, cm/s	U_{st}, cm/s
190	548.0	2600	1.0	100.0	125.0	186.10	.4	225.0	997.1	.894	71.97	12.03	11.80
191	548.0	2600	1.0	100.0	125.0	186.10	.4	225.0	997.1	.894	71.97	13.39	11.65
192	548.0	2600	1.0	49.8	25.0	40.14	.4	125.0	1025.7	1.221	71.70	7.95	7.95
193	548.0	2600	1.0	49.8	25.0	40.14	.4	125.0	1025.7	1.221	71.70	7.32	6.17
194	548.0	2600	1.0	49.8	50.0	73.72	.4	150.0	1025.7	1.221	71.70	11.09	6.74
195	548.0	2600	1.0	49.8	50.0	73.72	.4	150.0	1025.7	1.221	71.70	11.13	6.13
196	548.0	2600	1.0	49.8	75.0	115.97	.4	175.0	1025.7	1.221	71.70	15.08	7.38
197	548.0	2600	1.0	49.8	75.0	115.97	.4	175.0	1025.7	1.221	71.70	15.04	7.38
198	548.0	2600	1.0	49.8	100.0	154.98	.4	200.0	1025.7	1.221	71.76	19.40	11.13
199	548.0	2600	1.0	49.8	100.0	154.98	.4	200.0	1025.7	1.221	71.70	19.32	9.92
200	548.0	2600	1.0	49.8	125.0	187.38	.4	225.0	1025.7	1.221	71.70	19.48	12.54
201	548.0	2600	1.0	49.8	125.0	187.38	.4	225.0	1025.7	1.221	71.70	19.40	12.59
202	328.0	2600	1.0	49.8	20.0	25.63	.4	120.0	997.1	.894	71.97	3.60	5.27
203	328.0	2600	1.0	49.8	20.0	25.63	.4	120.0	997.1	.894	71.97	3.60	5.27
204	328.0	2600	1.0	49.8	20.0	25.63	.4	120.0	1025.7	1.221	71.70	4.15	5.27
205	328.0	2600	1.0	49.8	20.0	25.63	.4	120.0	1025.7	1.221	71.70	6.34	5.24
206	328.0	2600	1.0	49.8	20.0	25.63	.4	120.0	1058.0	1.810	70.97	4.73	5.23
207	328.0	2600	1.0	49.8	20.0	25.63	.4	120.0	1058.0	1.810	70.97	6.32	5.23
208	328.0	2600	1.0	49.8	20.0	25.63	.4	120.0	1085.3	2.653	70.11	4.13	3.57
209	328.0	2600	1.0	49.8	40.0	51.27	.4	140.0	997.1	.894	71.97	6.28	4.15
210	328.0	2600	1.0	49.8	40.0	51.27	.4	140.0	997.1	.894	71.97	6.90	0.00
211	328.0	2600	1.0	49.8	40.0	51.27	.4	140.0	997.1	.894	71.97	6.90	4.15
212	328.0	2600	1.0	49.8	40.0	51.27	.4	140.0	1025.7	1.221	71.70	5.80	3.58
213	328.0	2600	1.0	49.8	40.0	51.27	.4	140.0	1025.7	1.221	71.70	6.28	4.15
214	328.0	2600	1.0	49.8	40.0	51.27	.4	140.0	1050.4	1.644	71.13	5.23	4.15
215	328.0	2600	1.0	49.8	40.0	51.27	.4	140.0	1050.4	1.644	71.13	5.80	4.15
216	328.0	2600	1.0	49.8	40.0	51.27	.4	140.0	1073.5	2.235	70.42	5.23	4.15
217	328.0	2600	1.0	49.8	40.0	51.27	.4	140.0	1073.5	2.235	70.42	5.24	4.15
218	328.0	2600	1.0	49.8	40.0	51.27	.4	140.0	1097.2	3.181	69.77	5.23	4.15
219	328.0	2600	1.0	49.8	40.0	51.27	.4	140.0	1097.2	3.181	69.77	5.23	4.14
220	328.0	2600	1.0	49.8	57.0	76.90	.4	157.0	997.1	.894	71.97	7.35	5.19
221	328.0	2600	1.0	49.8	57.0	76.90	.4	157.0	997.1	.894	71.97	7.37	5.19
222	328.0	2600	1.0	49.8	57.0	76.90	.4	157.0	1025.7	1.221	71.71	6.85	4.68
223	328.0	2600	1.0	49.8	57.0	76.90	.4	157.0	1025.7	1.221	71.71	6.85	4.67
224	328.0	2600	1.0	49.8	57.0	76.90	.4	157.0	1050.4	1.644	71.15	5.75	4.11
225	328.0	2600	1.0	49.8	57.0	76.90	.4	157.0	1050.4	1.644	71.15	5.18	4.10
226	328.0	2600	1.0	49.8	57.0	76.90	.4	157.0	1081.4	2.502	70.23	4.66	3.54
227	328.0	2600	1.0	49.8	57.0	76.90	.4	157.0	1081.4	2.502	70.23	5.17	4.10
228	328.0	2600	1.0	49.8	57.0	76.90	.4	157.0	1107.9	3.787	69.35	4.65	2.49
229	328.0	2600	1.0	49.8	57.0	76.90	.4	157.0	1107.9	3.787	69.35	4.09	2.98
230	328.0	2600	1.0	49.8	74.0	102.54	.4	174.0	997.1	.894	71.97	9.03	5.20
231	328.0	2600	1.0	49.8	74.0	102.54	.4	174.0	997.1	.894	71.97	8.49	5.77
232	328.0	2600	1.0	49.8	74.0	102.54	.4	174.0	1025.7	1.221	71.70	7.38	4.68
233	328.0	2600	1.0	49.8	74.0	102.54	.4	174.0	1025.7	1.221	71.70	7.90	4.69
234	328.0	2600	1.0	49.8	74.0	102.54	.4	174.0	1053.0	1.699	71.06	6.32	4.11
235	328.0	2600	1.0	49.8	74.0	102.54	.4	174.0	1053.0	1.699	71.06	5.75	4.10
236	328.0	2600	1.0	49.8	74.0	102.54	.4	174.0	1086.6	2.706	70.07	5.19	4.10
237	328.0	2600	1.0	49.8	74.0	102.54	.4	174.0	1086.6	2.706	70.07	5.73	4.10
238	328.0	2600	1.0	49.8	74.0	102.54	.4	174.0	1115.9	4.367	69.06	4.66	2.98
239	328.0	2600	1.0	49.8	74.0	102.54	.4	174.0	1115.9	4.367	69.06	4.66	2.98
240	328.0	2600	1.0	49.8	94.0	128.17	.4	194.0	997.1	.894	71.97	9.63	6.42
241	328.0	2600	1.0	49.8	94.0	128.17	.4	194.0	997.1	.894	71.97	9.63	5.84
242	328.0	2600	1.0	49.8	94.0	128.17	.4	194.0	1025.7	1.221	71.71	8.04	4.75
243	328.0	2600	1.0	49.8	94.0	128.17	.4	194.0	1025.7	1.221	71.71	7.46	4.75
244	328.0	2600	1.0	49.8	94.0	128.17	.4	194.0	1053.0	1.699	71.09	6.42	4.19
245	328.0	2600	1.0	49.8	94.0	128.17	.4	194.0	1053.0	1.699	71.09	6.42	4.75
246	328.0	2600	1.0	49.8	94.0	128.17	.4	194.0	1080.1	2.455	70.26	5.27	4.16
247	328.0	2600	1.0	49.8	94.0	128.17	.4	194.0	1080.1	2.455	70.26	5.83	4.18
248	328.0	2600	1.0	49.8	94.0	128.17	.4	194.0	1110.6	3.967	69.30	5.27	3.07
249	328.0	2600	1.0	49.8	94.0	128.17	.4	194.0	1110.6	3.967	69.30	5.25	3.62
250	328.0	2600	1.0	49.8	113.0	153.80	.4	213.0	997.1	.894	71.97	11.73	6.57
251	328.0	2600	1.0	49.8	113.0	153.80	.4	213.0	997.1	.894	71.97	11.73	6.57
252	328.0	2600	1.0	49.8	113.0	153.80	.4	213.0	1025.7	1.221	71.70	9.08	4.05
253	328.0	2600	1.0	49.8	113.0	153.80	.4	213.0	1025.7	1.221	71.70	9.06	5.29
254	328.0	2600	1.0	49.8	113.0	153.80	.4	213.0	1053.0	1.699	71.06	7.84	4.06
255	328.0	2600	1.0	49.8	113.0	153.80	.4	213.0	1053.0	1.699	71.06	7.84	4.05

TABLE A1. (cont'd)

Test No.	D_p, mm	ρ_s, Kg/ms	Ψ	Dt, mm	H, mm	L, Kg/m^2	ϵ	H_ℓ, mm	ρ_ℓ, Kg/m^3	μ_ℓ, Cp	σ, dynes/cm	U_{mf}, cm/s	U_{st}, cm/s
256	328.0	2600	1.0	49.8	113.0	153.80	.4	213.0	1084.0	2.602	70.17	6.58	4.06
257	328.0	2600	1.0	49.8	113.0	153.80	.4	213.0	1084.0	2.602	70.17	5.88	4.01
258	328.0	2600	1.0	49.8	113.0	153.80	.4	213.0	1113.3	4.165	69.13	5.29	2.78
259	328.0	2600	1.0	49.8	113.0	153.80	.4	213.0	1113.3	4.165	69.13	5.29	2.78
260	328.0	2600	1.0	49.8	130.0	179.44	.4	260.0	997.1	.894	71.97	12.00	7.46
261	328.0	2600	1.0	49.8	130.0	179.44	.4	260.0	997.1	.894	71.97	12.02	7.46
262	328.0	2600	1.0	49.8	130.0	179.44	.4	260.0	1026.9	1.239	71.70	9.59	4.74
263	328.0	2600	1.0	49.8	130.0	179.44	.4	260.0	1026.9	1.239	71.70	9.59	5.29
264	328.0	2600	1.0	49.8	130.0	179.44	.4	260.0	1058.1	1.810	70.92	6.38	4.75
265	328.0	2600	1.0	49.8	130.0	179.44	.4	260.0	1058.1	1.810	70.92	6.38	4.74
266	328.0	2600	1.0	49.8	130.0	179.44	.4	260.0	1089.3	2.817	70.00	5.29	4.17
267	328.0	2600	1.0	49.8	130.0	179.44	.4	260.0	1089.3	2.817	70.00	5.29	4.17
268	328.0	2600	1.0	49.8	130.0	179.44	.4	260.0	1113.3	4.165	69.12	5.29	4.17
269	328.0	2600	1.0	49.8	130.0	179.44	.4	260.0	1113.3	4.165	69.12	5.29	3.61
270	11.0	10000	.7	49.8	25.0	128.17	.4	125.0	997.1	.894	71.97	4.63	0.00
271	11.0	10000	.7	49.8	50.0	256.34	.4	150.0	997.1	.894	71.97	3.00	0.00
272	11.0	10000	.7	49.8	75.0	384.51	.4	175.0	997.1	.894	71.97	5.23	0.00
273	11.0	10000	.7	49.8	110.0	512.68	.4	210.0	997.1	.894	71.97	5.35	0.00
274	11.0	10000	.7	49.8	130.0	640.85	.4	230.0	997.1	.894	71.97	5.44	0.00
275	79.0	10000	.7	49.9	20.0	85.36	.4	120.0	997.1	.894	71.97	42.38	0.00
276	311.0	8900	1.0	49.8	20.0	98.18	.4	120.0	1113.3	4.165	69.20	60.26	93.59
277	311.0	8900	1.0	49.8	20.0	97.41	.4	120.0	1113.3	4.165	69.20	47.32	21.50
278	311.0	8900	1.0	49.8	20.0	97.41	.4	120.0	1113.3	4.165	69.20	47.09	21.45
279	311.0	8900	1.0	49.8	40.0	194.82	.4	140.0	1113.3	4.165	69.20	51.14	21.16
280	311.0	8900	1.0	49.8	40.0	194.82	.4	140.0	1113.3	4.165	69.20	46.69	20.19
281	311.0	8900	1.0	49.8	60.0	292.23	.4	160.0	1113.3	4.165	69.20	53.62	21.46
282	311.0	8900	1.0	49.8	60.0	292.23	.4	160.0	1113.3	4.165	69.20	53.62	17.00
283	311.0	8900	1.0	49.8	80.0	389.64	.4	180.0	1113.3	4.165	69.20	61.69	21.67
284	311.0	8900	1.0	49.8	80.0	389.64	.4	180.0	1113.3	4.165	69.20	54.41	16.53
285	311.0	8900	1.0	49.8	20.0	97.41	.4	120.0	1165.0	12.360	67.14	54.41	21.37
286	311.0	8900	1.0	49.8	20.0	97.41	.4	120.0	1165.0	12.360	67.14	46.93	6.25
287	311.0	8900	1.0	49.8	40.0	194.82	.4	140.0	1165.0	12.360	67.14	54.41	4.65
288	311.0	8900	1.0	49.8	40.0	194.82	.4	140.0	1165.0	12.360	67.14	46.85	46.45
289	311.0	8900	1.0	49.8	60.0	292.23	.4	160.0	1165.0	12.360	67.14	40.34	4.62
290	311.0	8900	1.0	49.8	60.0	292.23	.4	160.0	1165.0	12.360	67.14	40.34	4.62
291	311.0	8900	1.0	49.8	80.0	389.64	.4	180.0	1165.0	12.360	67.14	14.32	4.12
292	311.0	8900	1.0	49.8	80.0	389.64	.4	180.0	1165.0	12.360	67.14	40.48	4.07
293	180.0	2600	1.0	49.8	25.0	41.27	.4	100.0	785.1	1.100	21.50	4.12	2.40
294	180.0	2600	1.0	49.8	25.0	41.27	.4	100.0	785.1	1.100	21.50	3.26	2.40
295	180.0	2600	1.0	49.8	50.0	81.97	.4	125.0	785.1	1.100	21.50	3.27	2.11
296	180.0	2600	1.0	49.8	50.0	81.97	.4	125.0	785.1	1.100	21.50	4.13	2.11
297	180.0	2600	1.0	49.8	50.0	81.97	.4	125.0	785.1	1.100	21.50	3.84	2.11
298	180.0	2600	1.0	49.8	75.0	113.51	.4	150.0	785.1	1.100	21.50	4.42	2.42
299	180.0	2600	1.0	49.8	75.0	113.51	.4	150.0	785.1	1.100	21.50	5.24	2.41
300	180.0	2600	1.0	49.8	75.0	113.51	.4	150.0	785.1	1.100	21.50	3.85	2.42
301	180.0	2600	1.0	49.8	100.0	156.83	.4	175.0	785.1	1.100	21.50	3.86	2.12
302	180.0	2600	1.0	49.8	100.0	156.83	.4	175.0	785.1	1.100	21.50	4.14	2.12
303	180.0	2600	1.0	49.8	125.0	197.69	.4	200.0	785.1	1.100	21.50	4.44	2.12
304	180.0	2600	1.0	49.8	125.0	197.69	.4	200.0	785.1	1.100	21.50	4.15	2.12
305	255.0	2600	1.0	49.8	25.0	41.53	.4	100.0	785.1	1.100	21.50	7.48	3.16
306	255.0	2600	1.0	49.8	25.0	41.53	.4	100.0	785.1	1.100	21.50	7.47	3.16
307	255.0	2600	1.0	49.8	50.0	76.54	.4	125.0	785.1	1.100	21.50	9.81	2.50
308	255.0	2600	1.0	49.8	50.0	76.54	.4	125.0	785.1	1.100	21.50	7.48	2.50
309	255.0	2600	1.0	49.8	50.0	76.54	.4	125.0	785.1	1.100	21.50	8.24	2.49
310	255.0	2600	1.0	49.8	75.0	108.69	.4	150.0	785.1	1.100	21.50	7.50	2.51
311	255.0	2600	1.0	49.8	75.0	108.69	.4	150.0	785.1	1.100	21.50	6.74	2.50
312	255.0	2600	1.0	49.8	100.0	146.73	.4	175.0	785.1	1.100	21.50	7.50	2.51
313	255.0	2600	1.0	49.8	100.0	146.73	.4	175.0	785.1	1.100	21.50	7.51	2.51
314	255.0	2600	1.0	49.8	125.0	182.41	.4	200.0	785.1	1.100	21.50	8.30	2.51
315	255.0	2600	1.0	49.8	125.0	182.41	.4	200.0	785.1	1.100	21.50	6.75	2.51
316	255.0	2600	1.0	49.8	125.0	182.41	.4	200.0	785.1	1.100	21.50	8.30	2.51
317	390.0	2600	1.0	49.8	25.0	41.89	.4	100.0	785.1	1.100	21.50	13.85	13.00
318	390.0	2600	1.0	49.8	25.0	41.89	.4	100.0	785.1	1.100	21.50	12.99	12.99
319	390.0	2600	1.0	49.8	50.0	73.77	.4	125.0	785.1	1.100	21.50	14.77	7.43
320	390.0	2600	1.0	49.8	50.0	73.77	.4	125.0	785.1	1.100	21.50	17.10	12.84
321	390.0	2600	1.0	49.8	75.0	107.71	.4	150.0	785.1	1.100	21.50	10.72	8.22
322	390.0	2600	1.0	49.8	75.0	107.71	.4	150.0	785.1	1.100	21.50	11.52	9.00
323	390.0	2600	1.0	49.8	100.0	146.73	.4	175.0	785.1	1.100	21.50	14.76	12.24
324	390.0	2600	1.0	49.8	100.0	146.73	.4	175.0	785.1	1.100	21.50	13.97	11.39
325	390.0	2600	1.0	49.8	125.0	185.74	.4	200.0	785.1	1.100	21.50	21.43	0.00
326	390.0	2600	1.0	49.8	125.0	185.74	.4	200.0	785.1	1.100	21.50	0.00	0.00
327	328.0	2600	1.0	49.8	25.0	38.96	.4	100.0	785.1	1.100	21.50	9.77	5.96
328	328.0	2600	1.0	49.8	25.0	38.96	.4	100.0	785.1	1.100	21.50	9.72	5.96
329	328.0	2600	1.0	49.8	50.0	80.49	.4	125.0	785.1	1.100	21.50	10.57	3.15
330	328.0	2600	1.0	49.8	50.0	80.49	.4	125.0	785.1	1.100	21.50	10.56	3.14
331	328.0	2600	1.0	49.8	75.0	119.20	.4	150.0	785.1	1.100	21.50	8.20	3.14
332	328.0	2600	1.0	49.8	75.0	119.20	.4	150.0	785.1	1.100	21.50	9.57	3.15
333	328.0	2600	1.0	49.8	100.0	168.88	.4	175.0	785.1	1.100	21.50	9.71	4.52
334	328.0	2600	1.0	49.8	100.0	168.88	.4	175.0	785.1	1.100	21.50	9.75	3.14
335	328.0	2600	1.0	49.8	125.0	200.05	.4	200.0	785.1	1.100	21.50	9.00	4.52
336	328.0	2600	1.0	49.8	125.0	200.05	.4	200.0	785.1	1.100	21.50	9.00	3.83
337	548.0	2600	1.0	49.8	25.0	43.22	.4	100.0	785.1	1.100	21.50	14.71	11.38
338	548.0	2600	1.0	49.8	25.0	43.22	.4	100.0	785.1	1.100	21.50	13.01	10.59
339	548.0	2600	1.0	49.8	50.0	83.31	.4	125.0	785.1	1.100	21.50	19.36	11.4[illegible]
340	548.0	2600	1.0	49.8	50.0	83.31	.4	125.0	785.1	1.100	21.50	18.56	9.59
341	548.0	2600	1.0	49.8	75.0	121.56	.4	150.0	785.1	1.100	21.50	20.38	13.36
342	548.0	2600	1.0	49.8	75.0	121.56	.4	150.0	785.1	1.100	21.50	19.08	12.30
343	548.0	2600	1.0	49.8	100.0	157.65	.4	175.0	785.1	1.100	21.50	25.46	17.57
344	548.0	2600	1.0	49.8	100.0	157.65	.4	175.0	785.1	1.100	21.50	25.59	14.77
345	548.0	2600	1.0	49.8	125.0	191.13	.4	200.0	785.1	1.100	21.50	28.72	23.75
346	548.0	2600	1.0	49.8	125.0	191.13	.4	200.0	785.1	1.100	21.50	28.04	23.70
347	463.0	2600	1.0	49.8	25.0	36.71	.4	100.0	785.1	1.100	21.50	16.91	14.71
348	463.0	2600	1.0	49.8	25.0	36.71	.4	100.0	785.1	1.100	21.50	13.08	11.35
349	463.0	2600	1.0	49.8	25.0	36.71	.4	100.0	785.1	1.100	21.50	12.27	10.59
350	463.0	2600	1.0	49.8	50.0	78.49	.4	125.0	785.1	1.100	21.50	18.44	13.11
351	463.0	2600	1.0	49.8	50.0	78.49	.4	125.0	785.1	1.100	21.50	17.17	13.08
352	463.0	2600	1.0	49.8	75.0	111.87	.4	150.0	785.1	1.100	21.50	21.99	16.03
353	463.0	2600	1.0	49.8	75.0	111.87	.4	150.0	785.1	1.100	21.50	21.99	13.22
354	463.0	2600	1.0	49.8	100.0	146.16	.4	175.0	785.1	1.100	21.50	23.67	17.21
355	463.0	2600	1.0	49.8	100.0	146.16	.4	175.0	785.1	1.100	21.50	23.62	16.17
356	255.0	2600	1.0	50.8	25.0	41.44	.4	75.0	785.1	1.100	21.50	8.67	5.56
357	255.0	2600	1.0	50.8	25.0	41.44	.4	75.0	785.1	1.100	21.50	8.66	5.54
358	255.0	2600	1.0	50.8	50.0	76.47	.4	100.0	785.1	1.100	21.50	8.73	5.55
359	255.0	2600	1.0	50.8	50.0	76.47	.4	100.0	785.1	1.100	21.50	7.11	5.54
360	255.0	2600	1.0	50.8	75.0	103.53	.4	125.0	785.1	1.100	21.50	8.68	5.56
361	255.0	2600	1.0	50.8	75.0	103.53	.4	125.0	785.1	1.100	21.50	8.70	5.56
362	255.0	2600	1.0	50.8	100.0	146.52	.4	150.0	785.1	1.100	21.50	8.71	5.56
363	255.0	2600	1.0	50.8	100.0	146.52	.4	150.0	785.1	1.100	21.50	7.11	5.60
364	255.0	2600	1.0	50.8	125.0	182.54	.4	175.0	785.1	1.100	21.50	8.78	5.59
365	255.0	2600	1.0	50.8	125.0	182.54	.4	175.0	785.1	1.100	21.50	7.17	5.58
366	327.5	2600	1.0	50.3	25.0	38.52	.4	75.0	785.1	1.100	21.50	10.34	8.21
367	327.5	2600	1.0	50.3	25.0	38.52	.4	75.0	785.1	1.100	21.50	10.30	9.27
368	327.5	2600	1.0	50.3	25.0	38.52	.4	75.0	785.1	1.100	21.50	10.33	8.15
369	327.5	2600	1.0	50.3	50.0	79.56	.4	100.0	785.1	1.100	21.50	11.62	9.32
370	327.5	2600	1.0	50.3	50.0	79.56	.4	100.0	785.1	1.100	21.50	11.65	9.45
371	327.5	2600	1.0	50.3	50.0	79.56	.4	100.0	785.1	1.100	21.50	12.79	10.45
372	327.5	2600	1.0	50.3	50.0	79.56	.4	100.0	785.1	1.100	21.50	11.69	10.53
373	327.5	2600	1.0	50.3	75.0	117.82	.4	125.0	785.1	1.100	21.50	12.93	9.27
374	327.5	2600	1.0	50.3	75.0	117.82	.4	125.0	785.1	1.100	21.50	14.93	10.46
375	327.5	2600	1.0	50.3	100.0	166.67	.4	150.0	785.1	1.100	21.50	18.01	15.37
376	327.5	2600	1.0	50.3	100.0	166.67	.4	150.0	785.1	1.100	21.50	18.42	11.68
377	327.5	2600	1.0	50.3	125.0	197.89	.4	175.0	785.1	1.100	21.50	19.78	11.76
378	327.5	2600	1.0	50.3	125.0	197.89	.4	175.0	785.1	1.100	21.50	19.84	13.77
379	327.5	2600	1.0	50.3	125.0	197.89	.4	175.0	785.1	1.100	21.50	21.04	18.29
380	462.5	2600	1.0	50.8	25.0	36.75	.4	75.0	785.1	1.100	21.50	17.88	15.15
381	462.5	2600	1.0	50.8	25.0	36.75	.4	75.0	785.1	1.100	21.50	18.02	15.36
382	462.5	2600	1.0	50.8	25.0	36.75	.4	75.0	785.1	1.100	21.50	17.02	15.30
383	462.5	2600	1.0	50.8	50.0	78.44	.4	100.0	785.1	1.100	21.50	20.93	18.21
384	462.5	2600	1.0	50.8	50.0	78.44	.4	100.0	785.1	1.100	21.50	20.99	18.28
385	462.5	2600	1.0	50.8	50.0	78.44	.4	100.0	785.1	1.100	21.50	20.83	15.36
386	462.5	2600	1.0	50.8	75.0	111.74	.4	125.0	785.1	1.100	21.50	21.36	18.60
387	462.5	2600	1.0	50.8	75.0	111.74	.4	125.0	785.1	1.100	21.50	21.49	18.60

TABLE A1. (cont'd)

Test No.	D_p, mm	ρ_s, Kg/ms	Ψ	Dt, mm	H, mm	L, Kg/m^2	ε	H_ℓ, mm	ρ_ℓ, Kg/m^3	μ_ℓ, Cp	σ, dynes/cm	U_{mf}, cm/s	U_{st}, cm/s
388	547.5	2600	1.0	50.3	25.0	42.80	.4	75.0	785.1	1.100	21.50	22.12	16.60
389	547.5	2600	1.0	50.3	50.0	82.33	.4	100.0	785.1	1.100	21.50	22.25	16.68
390	547.5	2600	1.0	50.3	50.0	82.33	.4	100.0	785.1	1.100	21.50	20.75	16.98
391	547.5	2600	1.0	50.3	75.0	117.41	.4	125.0	785.1	1.100	21.50	27.39	20.48
392	547.5	2600	1.0	50.3	75.0	117.41	.4	125.0	785.1	1.100	21.50	25.23	22.89
393	547.5	2600	1.0	50.8	100.0	152.94	.4	150.0	785.1	1.100	21.50	31.46	27.52
394	547.5	2600	1.0	50.8	100.0	152.94	.4	150.0	785.1	1.100	21.50	31.16	29.59
395	547.5	2600	1.0	50.8	125.0	185.25	.4	175.0	785.1	1.100	21.50	35.35	32.88
396	547.5	2600	1.0	50.8	125.0	185.25	.4	175.0	785.1	1.100	21.50	35.56	32.66